Aircraft Data for the Real-Time Flight Simulation

Author: Marek M. Cel
Revision: 5
Date: 2020-01-12

iii. publicity and privacy rights pertaining to a person's image or likeness depicted in a Work;
iv. rights protecting against unfair competition in regards to a Work, subject to the limitations in paragraph 4(a), below;
v. rights protecting the extraction, dissemination, use and reuse of data in a Work;
vi. database rights (such as those arising under Directive 96/9/EC of the European Parliament and of the Council of 11 March 1996 on the legal protection of databases, and under any national implementation thereof, including any amended or successor version of such directive); and
vii. other similar, equivalent or corresponding rights throughout the world based on applicable law or treaty, and any national implementations thereof.

2. Waiver. To the greatest extent permitted by, but not in contravention of, applicable law, Affirmer hereby overtly, fully, permanently, irrevocably and unconditionally waives, abandons, and surrenders all of Affirmer's Copyright and Related Rights and associated claims and causes of action, whether now known or unknown (including existing as well as future claims and causes of action), in the Work (i) in all territories worldwide, (ii) for the maximum duration provided by applicable law or treaty (including future time extensions), (iii) in any current or future medium and for any number of copies, and (iv) for any purpose whatsoever, including without limitation commercial, advertising or promotional purposes (the "Waiver"). Affirmer makes the Waiver for the benefit of each member of the public at large and to the detriment of Affirmer's heirs and successors, fully intending that such Waiver shall not be subject to revocation, rescission, cancellation, termination, or any other legal or equitable action to disrupt the quiet enjoyment of the Work by the public as contemplated by Affirmer's express Statement of Purpose.

3. Public License Fallback. Should any part of the Waiver for any reason be judged legally invalid or ineffective under applicable law, then the Waiver shall be preserved to the maximum extent permitted taking into account Affirmer's express Statement of Purpose. In addition, to the extent the Waiver is so judged Affirmer hereby grants to each affected person a royalty-free, non transferable, non sublicensable, non exclusive, irrevocable and unconditional license to exercise Affirmer's Copyright and Related Rights in the Work (i) in all territories worldwide, (ii) for the maximum duration provided by applicable law or treaty (including future time extensions), (iii) in any current or future medium and for any number of copies, and (iv) for any purpose whatsoever, including without limitation commercial, advertising or promotional purposes (the "License"). The License shall be deemed effective as of the date CC0 was applied by Affirmer to the Work. Should any part of the License for any reason be judged legally invalid or ineffective under applicable law, such partial invalidity or ineffectiveness shall not invalidate the remainder of the License, and in such case Affirmer hereby affirms that he or she will not (i) exercise any of his or her remaining Copyright and Related Rights in the Work or (ii) assert any associated claims and causes of action with respect to the Work, in either case contrary to Affirmer's express Statement of Purpose.

4. Limitations and Disclaimers.

a. No trademark or patent rights held by Affirmer are waived, abandoned, surrendered, licensed or otherwise affected by this document.
b. Affirmer offers the Work as-is and makes no representations or warranties of any kind concerning the Work, express, implied, statutory or otherwise, including without limitation warranties of title, merchantability, fitness for a particular purpose, non infringement, or the absence of latent or other defects, accuracy, or the present or absence of errors, whether or not discoverable, all to the greatest extent permissible under applicable law.
c. Affirmer disclaims responsibility for clearing rights of other persons that may apply to the Work or any use thereof, including without limitation any person's Copyright and Related Rights in the Work. Further, Affirmer disclaims responsibility for obtaining any necessary consents, permissions or other rights required for any use of the Work.
d. Affirmer understands and acknowledges that Creative Commons is not a party to this document and has no duty or obligation with respect to this CC0 or use of the Work.

Contents

Notation

$a = \dfrac{dC_L}{da}$	[1/rad] lift curve slope
$A = \dfrac{b^2}{S}$	[-] wing aspect ratio
b	[m] wing span
c_r	[m] chord at wing root
c_t	[m] chord at wing tip
$\hat{c}$, MAC	[m] mean aerodynamic chord
C_D	[-] drag coefficient
C_l	[-] rolling moment coefficient
C_L	[-] lift coefficient
C_m	[-] pitching moment coefficient
C_n	[-] yawing moment coefficient
C_Y	[-] side force coefficient
C_μ	[-] k-ε turbulence model constant
d	[m] fuselage diameter
D	[N] drag
e	[-] Oswald efficiency factor
i	[rad] incidence angle
I	[-] turbulence intensity
k	[$\mathrm{m}^2/\mathrm{s}^2$] turbulence kinetic energy
L	[N] lift
L	[m] reference length scale
p	[Pa] pressure
Re	[-] Reynolds number
S	[m^2] wing area
V	[m/s] velocity
α	[rad] angle of attack
β	[rad] angle of sideslip

$\lambda = \frac{c_t}{c_r}$	[-] wing taper ratio
Λ_{LE}	[rad] leading edge sweep angle
$\Lambda_{t/c}$	[rad] sweep angle at maximum thickness
ω	[1/s] specific turbulence dissipation rate
$\frac{\partial \epsilon}{\partial \alpha}$	[-] horizontal stabilizer downwash angle derivative with respect to the aircraft angle of attack

Chapter 1

Geometric Parameters

1.1 Wing Basic Geometric Parameters

Aspect ratio is given by the following formula: [1]

$$A = \frac{b^2}{S} \tag{1.1}$$

Taper ratio is given by the following formula. [1]

$$\lambda = \frac{c_t}{c_r} \tag{1.2}$$

1.2 Mean Aerodynamic Chord

For tapper wing mean aerodynamic chord can be calculated using following formula: [2, 3]

$$\hat{c} = \frac{2}{3} c_r \frac{1 + \lambda + \lambda^2}{1 + \lambda} \tag{1.3}$$

For more complex shapes mean aerodynamic chord is given as follows: [4]

$$\hat{c} = \left(\int_{-\frac{b}{2}}^{\frac{b}{2}} (c(y))^2 \, dy \right) \div \left(\int_{-\frac{b}{2}}^{\frac{b}{2}} (c(y)) \, dy \right) \tag{1.4}$$

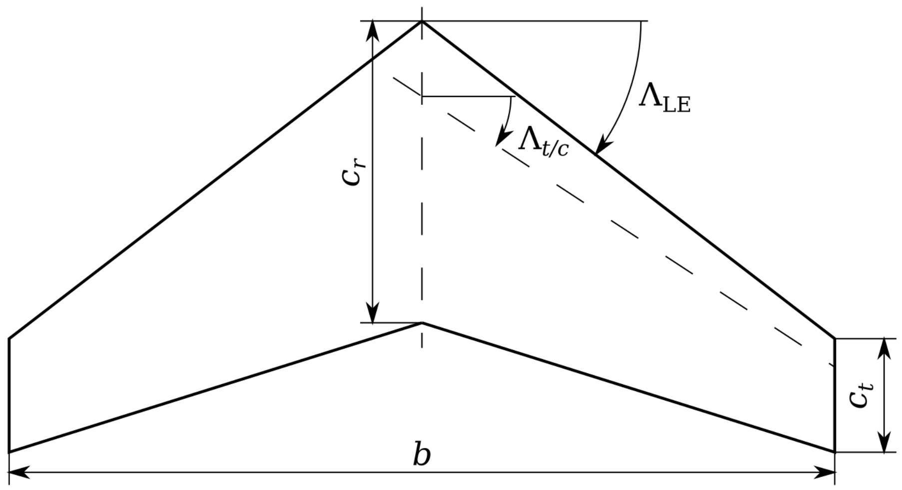

Figure 1.1: Wing basic geometric parameters

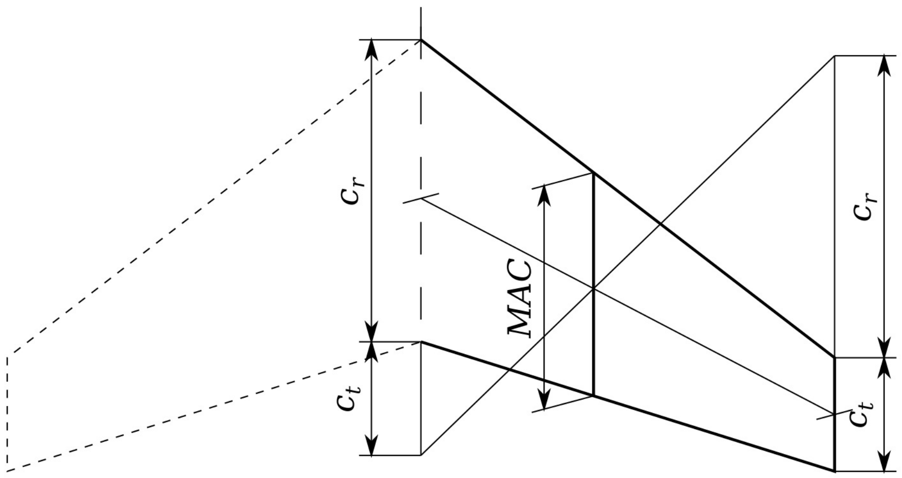

Figure 1.2: Mean aerodynamic chord

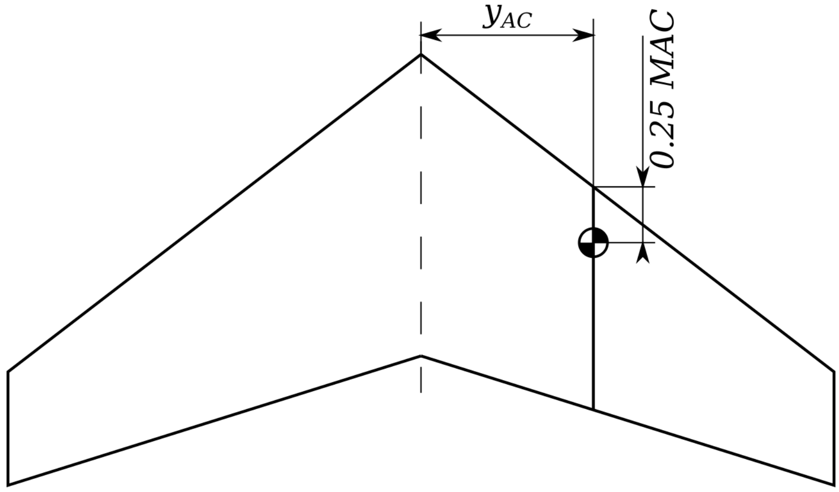

Figure 1.3: Wing aerodynamic center

1.3 Wing Aerodynamic Center

Position of wing aerodynamic center $\vec{r}_{AC}$ is at 25% of the mean aerodynamic chord and its lateral coordinate is given by the following formula. [1, 2, 3, 5]

$$y_{AC} = \frac{b\,(1 + 2\lambda)}{6\,(1 + \lambda)} \tag{1.5}$$

Chapter 2

Aerodynamic Characteristics

2.1 Aerodynamic Characteristics Approximation

2.1.1 Lift Coefficient Approximation

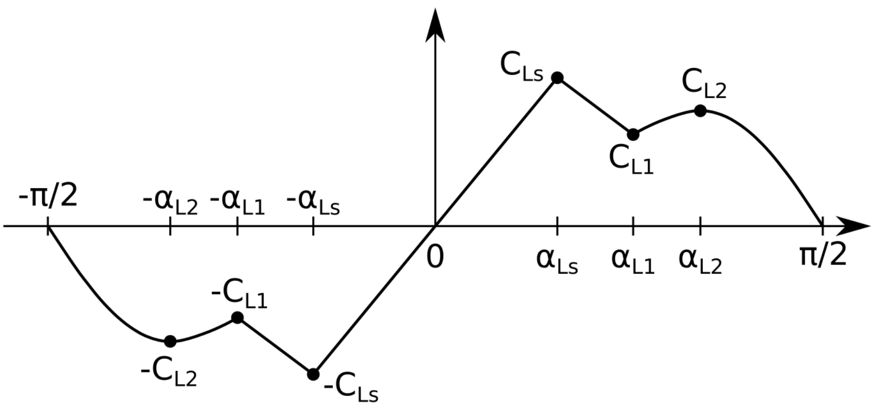

Figure 2.1: Lift coefficient approximation

Following approximation is used to get lift coefficient for the full range of angle of attack. [6]

Lift coefficient is given by the following expressions:

$$C_L = -\frac{(\alpha+\alpha_{L2})\left(\alpha+\frac{\pi}{2}\right)}{(\alpha_{L1}-\alpha_{L2})\left(\alpha_{L1}-\frac{\pi}{2}\right)}C_{L1} - \frac{(\alpha+\alpha_{L1})\left(\alpha+\frac{\pi}{2}\right)}{(\alpha_{L2}-\alpha_{L1})\left(\alpha_{L2}-\frac{\pi}{2}\right)}C_{L2} \quad \text{for } -\frac{\pi}{2} \le \alpha \le -\alpha_{L1} \tag{2.1}$$

$$C_L = \frac{C_{L1}-C_{Ls}}{\alpha_{L1}-\alpha_{Ls}}(\alpha+\alpha_{Ls}) - C_{Ls} \text{ for } -\alpha_{L1} < \alpha \le -\alpha_{Ls} \tag{2.2}$$

$$C_L = \frac{C_{Ls}}{\alpha_{Ls}}\alpha \text{ for } -\alpha_{Ls} < \alpha < \alpha_{Ls} \tag{2.3}$$

$$C_L = \frac{C_{L1}-C_{Ls}}{\alpha_{L1}-\alpha_{Ls}}(\alpha-\alpha_{Ls}) + C_{Ls} \text{ for } \alpha_{Ls} \le \alpha < \alpha_{L1} \tag{2.4}$$

$$C_L = \frac{(\alpha-\alpha_{L2})\left(\alpha-\frac{\pi}{2}\right)}{(\alpha_{L1}-\alpha_{L2})\left(\alpha_{L1}-\frac{\pi}{2}\right)}C_{L1} + \frac{(\alpha-\alpha_{L1})\left(\alpha-\frac{\pi}{2}\right)}{(\alpha_{L2}-\alpha_{L1})\left(\alpha_{L2}-\frac{\pi}{2}\right)}C_{L2} \quad \text{for } \alpha_{L1} \le \alpha \le \frac{\pi}{2} \tag{2.5}$$

2.1.2 Drag Coefficient Approximation

Following approximation is used to get drag coefficient for the full range of angle of attack. [6] Drag coefficient is assumed to be symmetric.

Drag coefficient is given by the following expressions:

$$C_D = \frac{(\alpha^2-\alpha_{D2}^2)(\alpha^2-\alpha_{D1}^2)}{\alpha_{D1}^2\alpha_{D2}^2}C_{D0} + \frac{(\alpha^2-\alpha_{D2}^2)\alpha^2}{(\alpha_{D1}^2-\alpha_{D2}^2)\alpha_{D1}^2}C_{D1} + \frac{(\alpha^2-\alpha_{D1}^2)\alpha^2}{(\alpha_{D2}^2-\alpha_{D1}^2)\alpha_{D2}^2}C_{D2} \quad \text{for } -\alpha_{D2} \le \alpha \le \alpha_{D2} \tag{2.6}$$

$$\begin{aligned} C_D = {} & \frac{(\alpha-\alpha_{D3})(\alpha-\alpha_{D4})\left(\alpha-\frac{\pi}{2}\right)}{(\alpha_{D2}-\alpha_{D3})(\alpha_{D2}-\alpha_{D4})\left(\alpha_{D2}-\frac{\pi}{2}\right)}C_{D2} \\ & + \frac{(\alpha-\alpha_{D2})(\alpha-\alpha_{D4})\left(\alpha-\frac{\pi}{2}\right)}{(\alpha_{D3}-\alpha_{D2})(\alpha_{D3}-\alpha_{D4})\left(\alpha_{D3}-\frac{\pi}{2}\right)}C_{D3} + \frac{(\alpha-\alpha_{D2})(\alpha-\alpha_{D3})\left(\alpha-\frac{\pi}{2}\right)}{(\alpha_{D4}-\alpha_{D2})(\alpha_{D4}-\alpha_{D3})\left(\alpha_{D4}-\frac{\pi}{2}\right)}C_{D4} \\ & + \frac{(\alpha-\alpha_{D2})(\alpha-\alpha_{D3})(\alpha-\alpha_{D4})}{\left(\frac{\pi}{2}-\alpha_{D2}\right)\left(\frac{\pi}{2}-\alpha_{D3}\right)\left(\frac{\pi}{2}-\alpha_{D4}\right)}C_{D5} \\ & \text{for } -\frac{\pi}{2} \le \alpha < -\alpha_{D2} \text{ and } \alpha_{D2} < \alpha \le \frac{\pi}{2} \end{aligned} \tag{2.7}$$

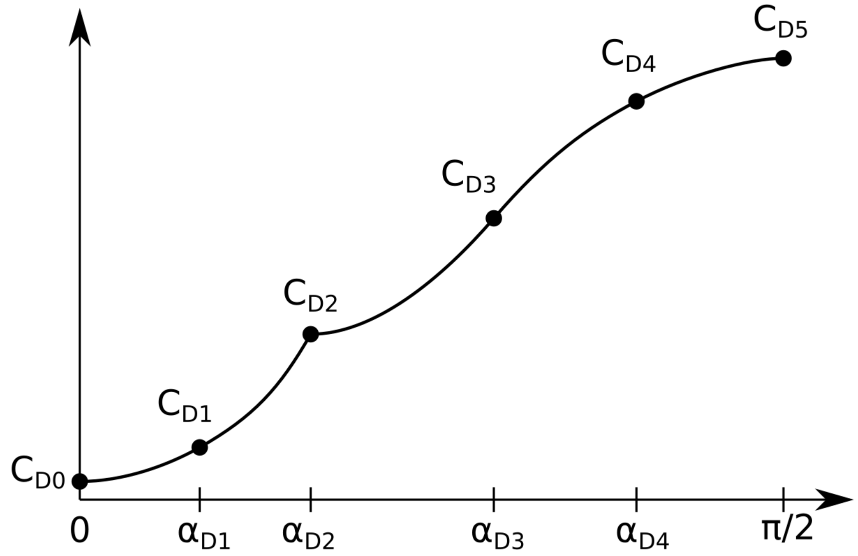

Figure 2.2: Drag coefficient approximation

Data available in [7] and [8] can be used to approximate aerodynamic characteristics outside linear range of the lift.

2.2 Finite Wing Aerodynamic Characteristics

Aerodynamic characteristics of the finite wing can be estimated within linear range of the lift.

Lift curve slope is given as follows: [2]

$$\frac{dC_L}{d\alpha} = \frac{2\pi A}{2 + \sqrt{4 + A^2\left(1 + \tan^2 \Lambda_{t/c}\right)}} \tag{2.8}$$

The finite wing lift coefficient within linear range is given by the following formula: [2]

$$C_L = C_{L\alpha=0} + \frac{dC_L}{d\alpha}\alpha \tag{2.9}$$

The finite wing maximum lift coefficient is given by: [1]

$$C_{L,max} = 0.9 C_{L,max\infty} \cos \Lambda_{t/c} \tag{2.10}$$

The finite wing drag coefficient is given as follows. [2]

$$C_D = C_{D0} + \frac{C_L^2}{\pi A e} \tag{2.11}$$

2.3 Horizontal Tail Incidence

Equilibrium of moments acting on an aircraft is given by the following equation:

$$r_{CG} mg + \frac{1}{2}\rho V^2 S\hat{c} C_m = l_h \frac{1}{2}\rho V^2 S_h C_{L,h} \tag{2.12}$$

Horizontal stabilizer lift coefficient is given as follows:

$$C_{L,h} = \left(\alpha + i_h - \alpha\frac{\partial\epsilon}{\partial\alpha}\right)\frac{dC_{L,h}}{d\alpha} \tag{2.13}$$

Where downwash derivative is given as: [9]

$$\frac{\partial\epsilon}{\partial\alpha} = \frac{2a}{\pi A} \tag{2.14}$$

Substituting equation (2.13) into (2.12) gives:

$$r_{CG} mg + \frac{1}{2}\rho V^2 S\hat{c} C_m = l_h \frac{1}{2}\rho V^2 S_h \left(\alpha + i_h - \alpha\frac{\partial\epsilon}{\partial\alpha}\right)\frac{dC_{L,h}}{d\alpha} \tag{2.15}$$

Solving this equation for horizontal tail incidence angle gives:

$$i_h = \frac{2 r_{CG} mg + \rho V^2 S\hat{c} C_m}{l_h \rho V^2 S_h \dfrac{dC_{L,h}}{d\alpha}} - \alpha\left(1 - \frac{\partial\epsilon}{\partial\alpha}\right) \tag{2.16}$$

Equilibrium of forces acting on an aircraft in level flight is given by the following equation:

$$mg = \frac{1}{2}\rho V^2 S C_L \tag{2.17}$$

Aircraft lift coefficient is given as follows:

$$C_L = C_{L0} + \alpha\frac{dC_L}{d\alpha} \tag{2.18}$$

Substituting equation (2.18) into (2.17) gives:

$$mg = \frac{1}{2}\rho V^2 S \left(C_{L0} + \alpha \frac{dC_L}{d\alpha} \right) \tag{2.19}$$

Solving this equation for angle of attack gives:

$$\alpha = \frac{2mg - \rho V^2 S C_{L0}}{\rho V^2 S \frac{dC_L}{d\alpha}} \tag{2.20}$$

Substituting equation (2.20) into (2.16) gives:

$$i_h = \frac{2r_{CG}mg + \rho V^2 S\hat{c}C_m}{l_h \rho V^2 S_h \frac{dC_{L,h}}{d\alpha}} - \frac{2mg - \rho V^2 S C_{L0}}{\rho V^2 S \frac{dC_L}{d\alpha}} \left(1 - \frac{\partial \epsilon}{\partial \alpha} \right) \tag{2.21}$$

2.4 Critical Angle of Attack

Equilibrium of forces acting on an aircraft in level flight is given by the following equation:

$$mg = \frac{1}{2}\rho V^2 \left(SC_L + S_h C_{L,h} \right) \tag{2.22}$$

As conventional configuration airplanes have horizontal stabilizer negative incidence angle, it is assumed that horizontal stabilizer is within its lift linear range when maximum lift coefficient is reached.

$$mg = \frac{1}{2}\rho V^2 \left[SC_L + S_h \left(\alpha_{cr} + i_h - \alpha_{cr} \frac{\partial \epsilon}{\partial \alpha} \right) \frac{dC_{L,h}}{d\alpha} \right] \tag{2.23}$$

Solving this equation for the maximum lift coefficient gives:

$$C_{L,max} = \frac{mg - \frac{1}{2}\rho V_{stall}^2 S_h \left(\alpha_{cr} + i_h - \alpha_{cr} \frac{\partial \epsilon}{\partial \alpha} \right) \frac{dC_{L,h}}{d\alpha}}{\frac{1}{2}\rho V_{stall}^2 S} \tag{2.24}$$

Assuming that maximum lift coefficient is within linear range:

$$C_{L,max} = C_{L0} + \alpha_{cr}\frac{dC_L}{d\alpha} \tag{2.25}$$

Substituting equation (2.25) into (2.24) gives:

$$C_{L0} + \alpha_{cr}\frac{dC_L}{d\alpha} = \frac{mg - \frac{1}{2}\rho V_{stall}^2 S_h \left(\alpha_{cr} + i_h - \alpha_{cr}\frac{\partial\epsilon}{\partial\alpha}\right)\frac{dC_{L,h}}{d\alpha}}{\frac{1}{2}\rho V_{stall}^2 S} \tag{2.26}$$

Solving this equation for critical angle of attack gives

$$\alpha_{cr} = \frac{2mg - \rho V_{stall}^2\left(S_h i_h \frac{dC_{L,h}}{d\alpha} + S C_{L0}\right)}{\rho V_{stall}^2\left[S\frac{dC_L}{d\alpha} + S_h\left(1 - \frac{\partial\epsilon}{\partial\alpha}\right)\frac{dC_{L,h}}{d\alpha}\right]} \tag{2.27}$$

Chapter 3

Mass and Inertia Data

3.1 Structure Groups Breakdown

Inertia tensor and center of mass coordinates can be estimated by breaking down empty aircraft into structure groups and then estimating their weights, inertia moments and coordinates, e.g. using aircraft drawing. [5]

3.2 OpenVSP

Mass Properties tool of the OpenVSP can be used to compute aircraft center of mass position and inertia tensor.

Chapter 4

Computational Fluid Dynamics

4.1 Tools

4.1.1 XFOIL

XFOIL is a program for the analysis of subsonic isolated airfoils developed at the Massachusetts Institute of Technology.

4.1.2 VSPAERO

VSPAERO is a combined vortex lattice method (VLM) and panel method solver integrated with OpenVSP, a parametric aircraft geometry tool developed at NASA Ames Research Center. VSPAERO can be used to compute aircraft aerodynamic characteristics within linear range of the lift. [10] OpenVSP allows users to fast create an aircraft 3D model by defining geometric parameters.

4.1.3 OpenFOAM

OpenFOAM is an open source software for computational fluid dynamics (CFD) originally created at Imperial College London. OpenFOAM contains various solvers intended to simulate different physical phenomena.

4.2 Workflow

4.2.1 XFOIL

Follow this steps to obtain airfoil characteristics. Notice that XFOIL commands are case sensitive. [11]

1. Open terminal and execute `xfoil` program.
   XFOIL command promt should start.
2. Read buffer airfoil from coordinate file with `LOAD` command e.g `LOAD 2412.dat`, or set NACA 4 or 5 digit airfoil with NACA command e.g. `NACA 2412`.
   Coordinate file is a simple text file which contains list of the 2D airfoil coordinate points starting at the trailing edge, progressing to the leading edge along the upper surface, and returning to the trailing edge along the lower surface.
3. Set number of panel nodes to at least 160 with `PPAR` command if necessary.
4. Enter operation mode with `OPER` command. `OPERi` indicates inviscid mode.
5. Enter viscous mode with `Visc` command.
   Enter Reynolds number for typical flight conditions. `OPERv` should appear.
6. Set Mach number for typical flight conditions with `Mach` command.
7. Specify output files with `Pacc` command.
8. Specify the angle of attack range and run computations with `Aseq` command.

4.2.2 VSPAERO

An appropriately define aircraft 3D model is needed to analyze. [12] Based on this model degenerated geometry file is generated for the vortex lattice method and surface triangulation file for the panel method.

VSPAERO can be run from within Analysis menu of the OpenVSP. Some additional setup should be done to start computations. Vortex lattice method or panel method solver should be chosen. Reference area, lengths and moment reference position should be specified to get correct results. Angle of attack range

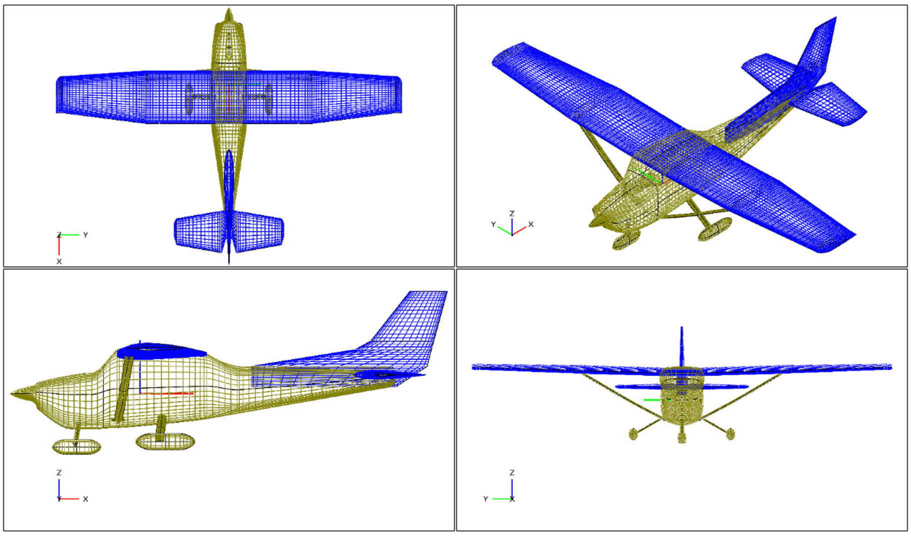

Figure 4.1: OpenVSP aircraft model

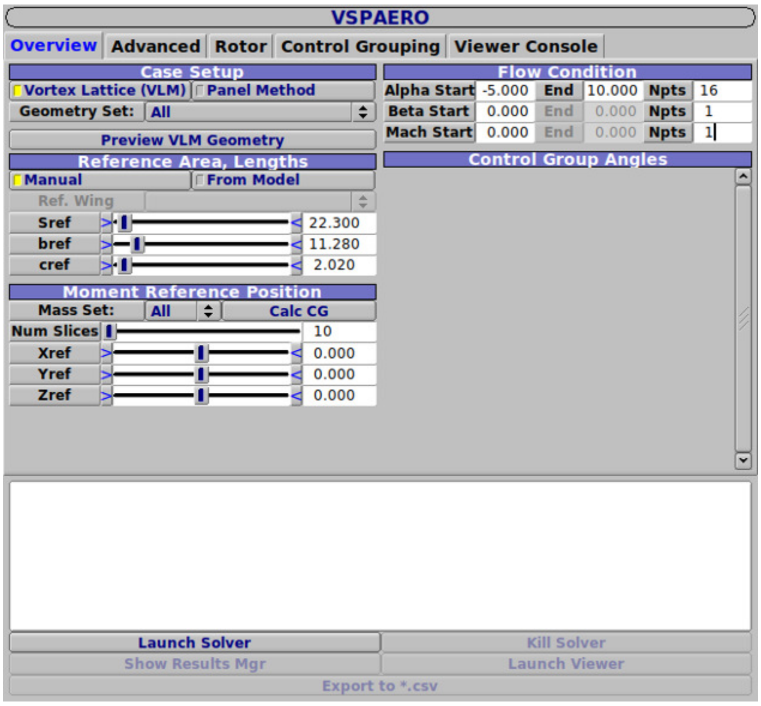

Figure 4.2: VSPAERO computations setup GUI

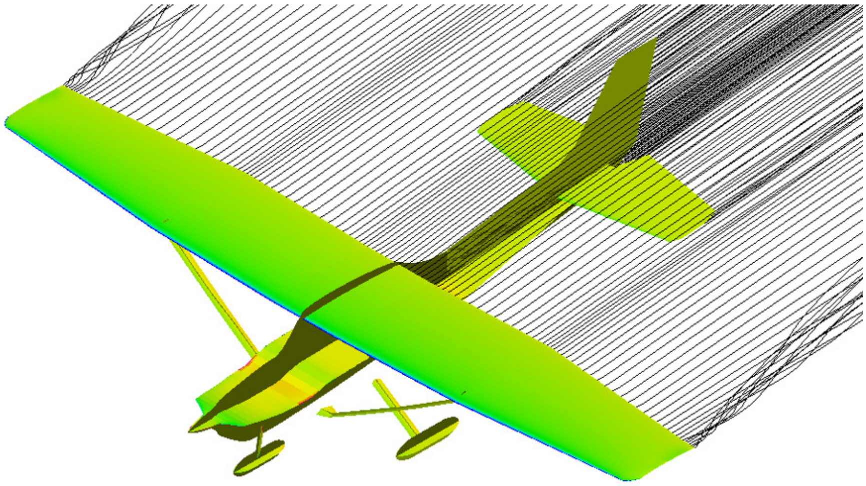

Figure 4.3: Wakes and pressure coefficient change distribution

should be specified for the linear range of the lift. Critical angle of attack can be calculated using formula (2.27). Mach number should be set to typical flight conditions.

VSPAERO Viewer and Results Manager can be used to visualize results. Computed aerodynamic characteristics are saved as plain text files, which are both easy to understand by a human and easy to read by a computer program.

4.2.3 OpenFOAM

Solver

OpenFOAM `simpleFoam` is a steady-state solver for incompressible, turbulent flow using SIMPLE (Semi-Implicit Method for Pressure Linked Equations) algorithm, which can be used to compute aircraft aerodynamic characteristics for the full range of angle of attack. [13, 14, 15]

SST k-ω Reynolds-Averaged Navier-Stokes (RANS) turbulence model is used.

Mesh – Control Volume

OpenFOAM `blockMesh` utility is used to create control volume mesh defined in `system/blockMeshDict` dictionary file as a mesh composed of hexahedral blocks.

The simplest case is when the control volume is defined by exactly one rectangular prisms.

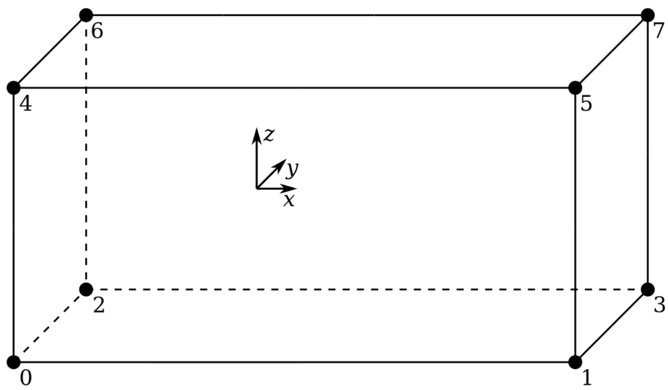

Figure 4.4: Basic control volume scheme

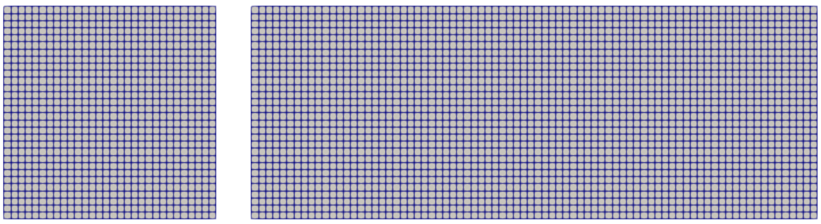

Figure 4.5: Basic control volume mesh

Dictionary file is listed below:

```
FoamFile
{
    version   2.0;
    format    ascii;
    class     dictionary;
    object    blockMeshDict;
}

cv_x_min -20.0;
cv_x_max  60.0;
cv_y_min -15.0;
```

```
cv_y_max  15.0;
cv_z_min -15.0;
cv_z_max  15.0;

convertToMeters 1.0;

vertices
(
  ( $cv_x_min $cv_y_min $cv_z_min )
  ( $cv_x_max $cv_y_min $cv_z_min )
  ( $cv_x_min $cv_y_max $cv_z_min )
  ( $cv_x_max $cv_y_max $cv_z_min )
  ( $cv_x_min $cv_y_min $cv_z_max )
  ( $cv_x_max $cv_y_min $cv_z_max )
  ( $cv_x_min $cv_y_max $cv_z_max )
  ( $cv_x_max $cv_y_max $cv_z_max )
);

blocks
(
  hex ( 0 1 3 2 4 5 7 6 ) ( 80 30 30 ) simpleGrading ( 1 1 1 )
);

edges
(
);

boundary
(
  inlet
  {
    type patch;
    faces
    (
      ( 0 4 6 2 )
    );
  }

  outlet
  {
    type patch;
    faces
    (
      ( 1 3 7 5 )
    );
  }

  walls
```

```
  {
    type patch;
    faces
    (
      ( 0 1 5 4 ) // left
      ( 2 6 7 3 ) // right
      ( 0 2 3 1 ) // bottom
      ( 4 5 7 6 ) // top
    );
  }
);

mergePatchPairs
(
);
```

Mesh – Simple Grading

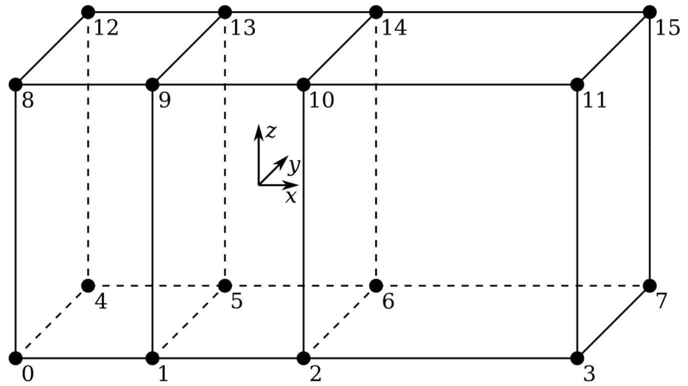

Figure 4.6: Graded control volume scheme

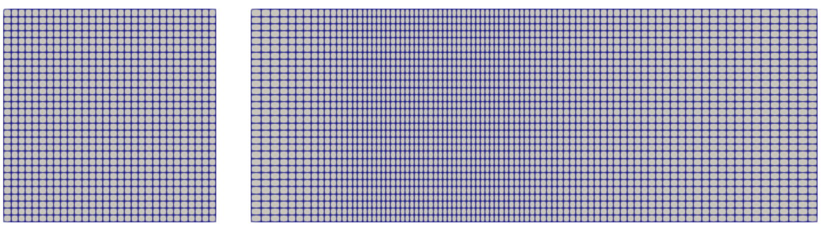

Figure 4.7: Graded control volume mesh

Grading is used to increase mesh resolution in regions of interest. Due to create graded control volume mesh it has to be divided into subdomains. Scheme of control volume mesh one dimension grading is presented below.

Dictionary file is listed below:

```
FoamFile
{
  version   2.0;
  format    ascii;
  class     dictionary;
  object    blockMeshDict;
}

cv_x_min -20.0;
cv_x_max  60.0;
cv_y_min -15.0;
cv_y_max  15.0;
cv_z_min -15.0;
cv_z_max  15.0;
s2_x_min  -5.0;
s2_x_max  15.0;

convertToMeters 1.0;

vertices
(
  ( $cv_x_min $cv_y_min $cv_z_min )
  ( $s2_x_min $cv_y_min $cv_z_min )
  ( $s2_x_max $cv_y_min $cv_z_min )
  ( $cv_x_max $cv_y_min $cv_z_min )
  ( $cv_x_min $cv_y_max $cv_z_min )
  ( $s2_x_min $cv_y_max $cv_z_min )
  ( $s2_x_max $cv_y_max $cv_z_min )
  ( $cv_x_max $cv_y_max $cv_z_min )
  ( $cv_x_min $cv_y_min $cv_z_max )
  ( $s2_x_min $cv_y_min $cv_z_max )
  ( $s2_x_max $cv_y_min $cv_z_max )
  ( $cv_x_max $cv_y_min $cv_z_max )
  ( $cv_x_min $cv_y_max $cv_z_max )
  ( $s2_x_min $cv_y_max $cv_z_max )
  ( $s2_x_max $cv_y_max $cv_z_max )
  ( $cv_x_max $cv_y_max $cv_z_max )
);

blocks
(
  hex ( 0  1  5  4  8  9 13 12 ) ( 15 30 30 )
```

```
    simpleGrading ( 0.5 1.0 1.0 )
  hex ( 1  2  6  5  9 10 14 13 ) ( 30 30 30 )
    simpleGrading ( 1.0 1.0 1.0 )
  hex ( 2  3  7  6 10 11 15 14 ) ( 45 30 30 )
    simpleGrading ( 2.0 1.0 1.0 )
);

edges
(
);

boundary
(
  inlet
  {
    type patch;
    faces
    (
      ( 0 8 12 4 )
    );
  }

  outlet
  {
    type patch;
    faces
    (
      ( 3 7 15 11 )
    );
  }

  walls
  {
    type patch;
    faces
    (
      // left
      (  0  1  9  8 )
      (  1  2 10  9 )
      (  2  3 11 10 )
      // right
      (  4 12 13  5 )
      (  5 13 14  6 )
      (  6 14 15  7 )
      // bottom
      (  0  4  5  1 )
      (  1  5  6  2 )
      (  2  6  7  3 )
```

```
      // top
      (  8  9 13 12 )
      (  9 10 14 13 )
      ( 10 11 15 14 )
    );
  }
);

mergePatchPairs
(
);
```

Mesh – Complex Grading

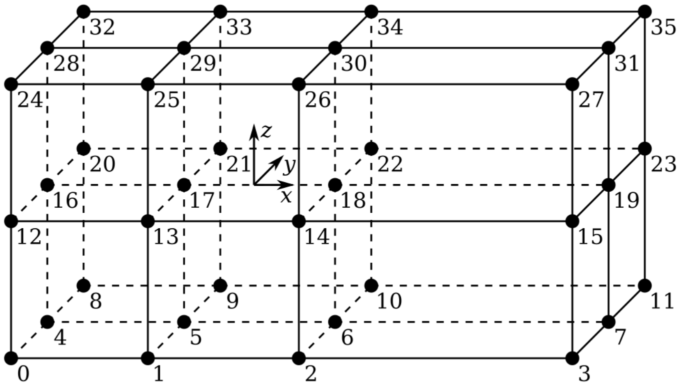

Figure 4.8: Complex graded control volume scheme

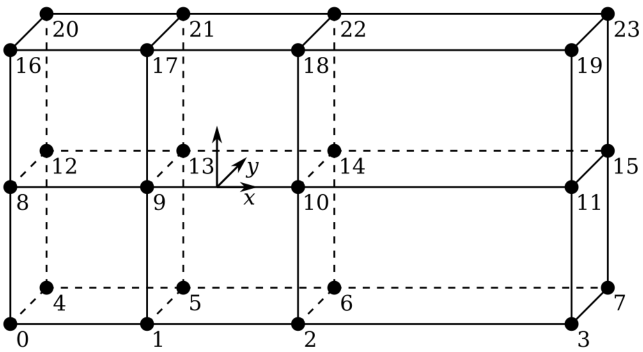

Figure 4.9: Symmetric control volume scheme

Scheme of complex control volume mesh grading is presented on figure 4.8.

For symmetric cases only half of the geometry can be considered to reduce computation time.

Dictionary file is listed below:

```
FoamFile
{
  version   2.0;
  format    ascii;
  class     dictionary;
  object    blockMeshDict;
}

cv_x_min -20.0;
cv_x_max  60.0;
cv_y_min -15.0;
cv_y_max  15.0;
cv_z_min -15.0;
cv_z_max  15.0;

s2_x_min  -5.0;
s2_x_max  15.0;

convertToMeters 1.0;

vertices
(
  ( $cv_x_min       0.0 $cv_z_min )
  ( $s2_x_min       0.0 $cv_z_min )
  ( $s2_x_max       0.0 $cv_z_min )
  ( $cv_x_max       0.0 $cv_z_min )
  ( $cv_x_min $cv_y_max $cv_z_min )
  ( $s2_x_min $cv_y_max $cv_z_min )
  ( $s2_x_max $cv_y_max $cv_z_min )
  ( $cv_x_max $cv_y_max $cv_z_min )
  ( $cv_x_min       0.0       0.0 )
  ( $s2_x_min       0.0       0.0 )
  ( $s2_x_max       0.0       0.0 )
  ( $cv_x_max       0.0       0.0 )
  ( $cv_x_min $cv_y_max       0.0 )
  ( $s2_x_min $cv_y_max       0.0 )
  ( $s2_x_max $cv_y_max       0.0 )
  ( $cv_x_max $cv_y_max       0.0 )
  ( $cv_x_min       0.0 $cv_z_max )
  ( $s2_x_min       0.0 $cv_z_max )
  ( $s2_x_max       0.0 $cv_z_max )
```

```
  ( $cv_x_max        0.0 $cv_z_max )
  ( $cv_x_min $cv_y_max $cv_z_max )
  ( $s2_x_min $cv_y_max $cv_z_max )
  ( $s2_x_max $cv_y_max $cv_z_max )
  ( $cv_x_max $cv_y_max $cv_z_max )
);

blocks
(
  hex (  0  1  5  4  8  9 13 12 ) ( 15 15 15 )
    simpleGrading ( 0.5 2.0 0.5 )
  hex (  8  9 13 12 16 17 21 20 ) ( 15 15 15 )
    simpleGrading ( 0.5 2.0 2.0 )
  hex (  1  2  6  5  9 10 14 13 ) ( 30 15 15 )
    simpleGrading ( 1.0 2.0 0.5 )
  hex (  9 10 14 13 17 18 22 21 ) ( 30 15 15 )
    simpleGrading ( 1.0 2.0 2.0 )
  hex (  2  3  7  6 10 11 15 14 ) ( 45 15 15 )
    simpleGrading ( 2.0 2.0 0.5 )
  hex ( 10 11 15 14 18 19 23 22 ) ( 45 15 15 )
    simpleGrading ( 2.0 2.0 2.0 )
);

edges
(
);

boundary
(
  inlet
  {
    type patch;
    faces
    (
      (  0  8 12  4 )
      (  8 16 20 12 )
    );
  }

  outlet
  {
    type patch;
    faces
    (
      (  3  7 15 11 )
      ( 11 15 23 19 )
    );
  }
```

```
  sym
  {
    type symmetryPlane;
    faces
    (
      // left
      (  0  1  9  8 )
      (  8  9 17 16 )
      (  1  2 10  9 )
      (  9 10 18 17 )
      (  2  3 11 10 )
      ( 10 11 19 18 )
    );
  }

  walls
  {
    type patch;
    faces
    (
      // right
      (  4 12 13  5 )
      ( 12 20 21 13 )
      (  5 13 14  6 )
      ( 13 21 22 14 )
      (  6 14 15  7 )
      ( 14 22 23 15 )

      // bottom
      (  0  4  5  1 )
      (  1  5  6  2 )
      (  2  6  7  3 )

      // top
      ( 16 17 21 20 )
      ( 17 18 22 21 )
      ( 18 19 23 22 )
    );
  }
);

mergePatchPairs
(
);
```

Mesh – Aircraft Geometry Model

OpenVSP can be used to create aircraft 3D model and export it to STL. OpenFOAM `snappyHexMesh` utility is used to combine control volume mesh with aircraft geometry model. Volume near aircraft geometry can be refined due to achieve better results. Meshing parameters are specified in `system/snappyHexMeshDict` file.

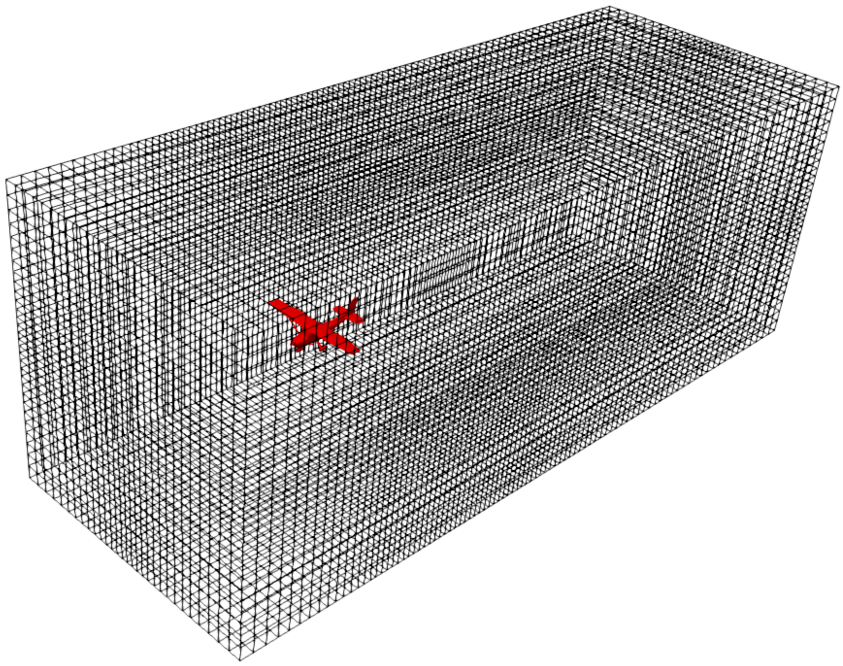

Figure 4.10: OpenFOAM complete mesh

Initial and Boundary Conditions

The inlet boundary conditions are given as follows. [16]

$$k = \frac{3}{2}\left(IV\right)^2 \tag{4.1}$$

$$\omega = \frac{k^{0.5}}{C_\mu L} \tag{4.2}$$

Where: [14, 15, 17, 18, 19]

$$I = 0.16Re^{-1/8} \tag{4.3}$$

$$C_\mu = 0.09 \tag{4.4}$$

Control

Notice that, as this is a steady-state simulation, time should be treated rather as iteration parameter rather than as a physical time. Maximum number of iterations in set `system/controlDict` dictionary file, `endTime` is a maximum number of iterations when `deltaT` is 1.

Solution

Case solving is terminated when pressure, velocity, turbulent kinetic energy and specific turbulence dissipation rate initial residual of the field equations falls below threshold values defined in `residualControl` dictionary in `system/fvSolution` file.

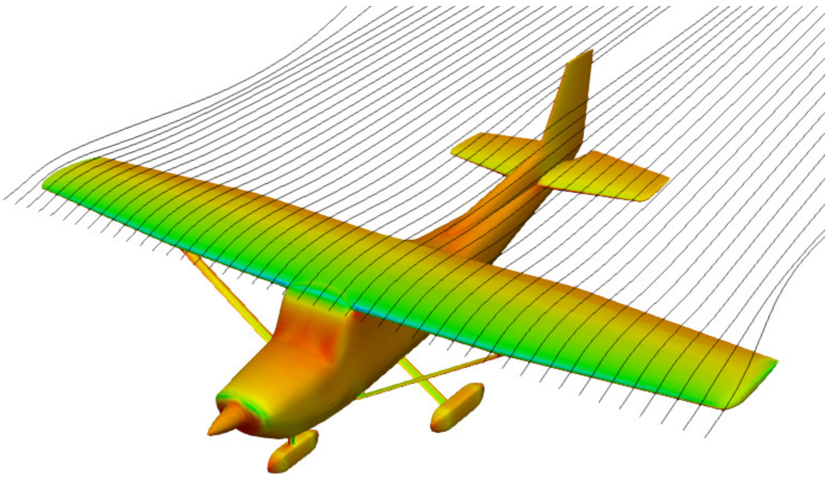

Figure 4.11: Streamlines and kinematic pressure distribution

If divergent or unstable behavior is observed decreasing under-relaxation factors defined in `relaxationFactors` dictionary in `system/fvSolution` file may improve solution convergence.

Physical quantity	Under-Relaxation Factor
Kinematic pressure	0.2 – 0.3
Velocity	0.5 – 0.7
Turbulent kinetic energy	0.5 – 0.7
Turbulence dissipation rate	0.5 – 0.7

Table 4.1: Commonly used under-relaxation factors [19, 20]

4.3 Results

4.3.1 XFOIL

XFOIL computations results, compared to the data available in [7] and [8], are shown in figures 4.12, 4.13 and 4.14.

4.3.2 VSPAERO

VSPAERO computations results, compared to the OpenFOAM computations results, are shown in figures 4.15, 4.16 and 4.17.

4.3.3 OpenFOAM

OpenFOAM computations results, compared to the data available in [21], are shown in figures 4.18 and 4.19.

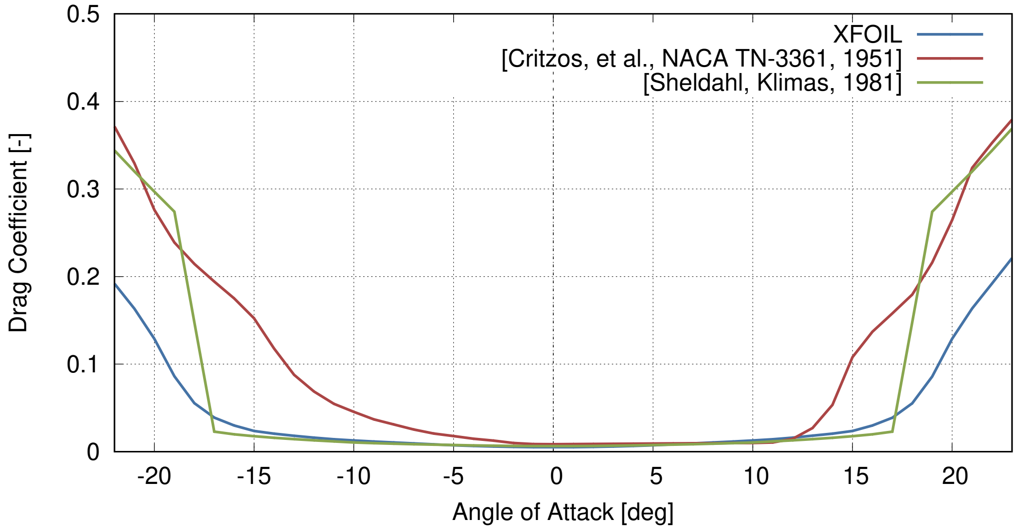

Figure 4.12: NACA 0012 drag coefficient

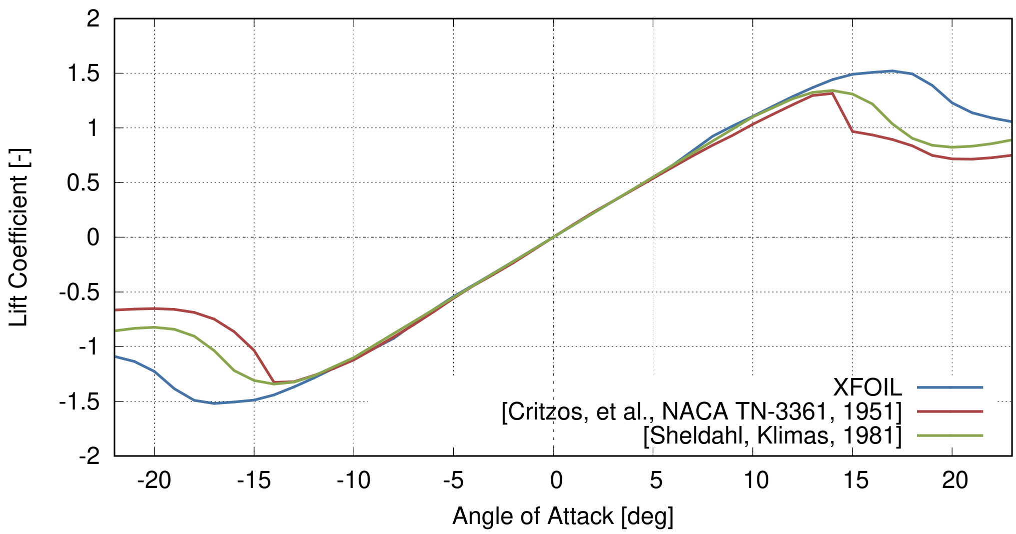

Figure 4.13: NACA 0012 lift coefficient

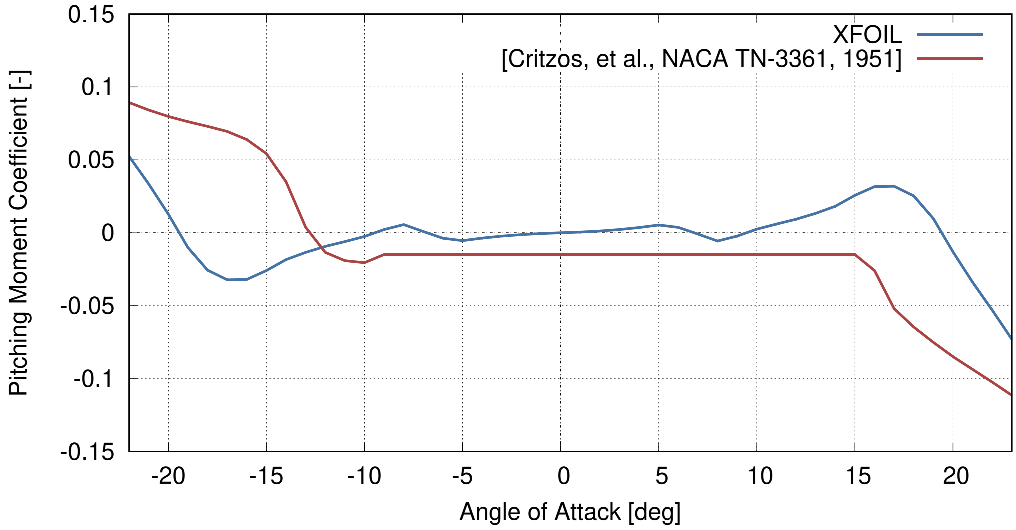

Figure 4.14: NACA 0012 pitching moment coefficient

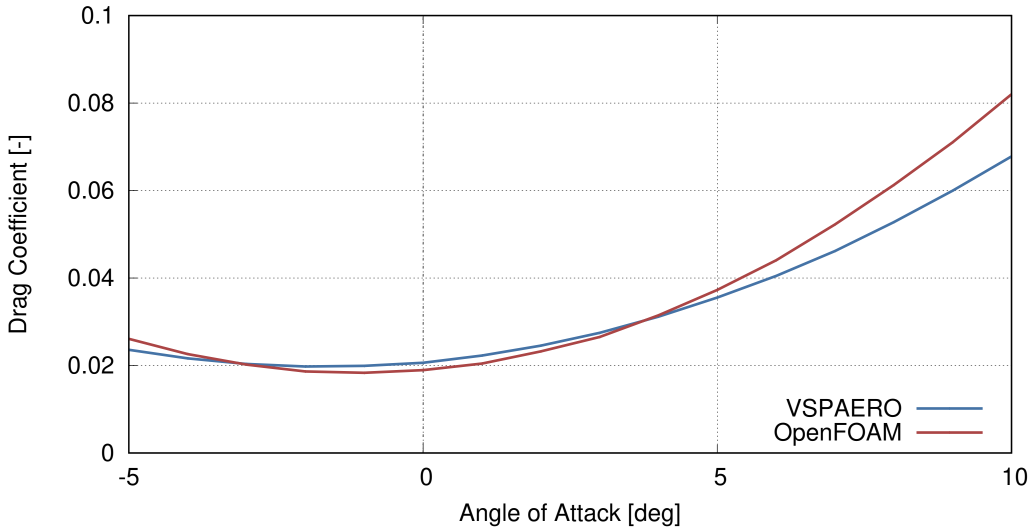

Figure 4.15: P-51 drag coefficient

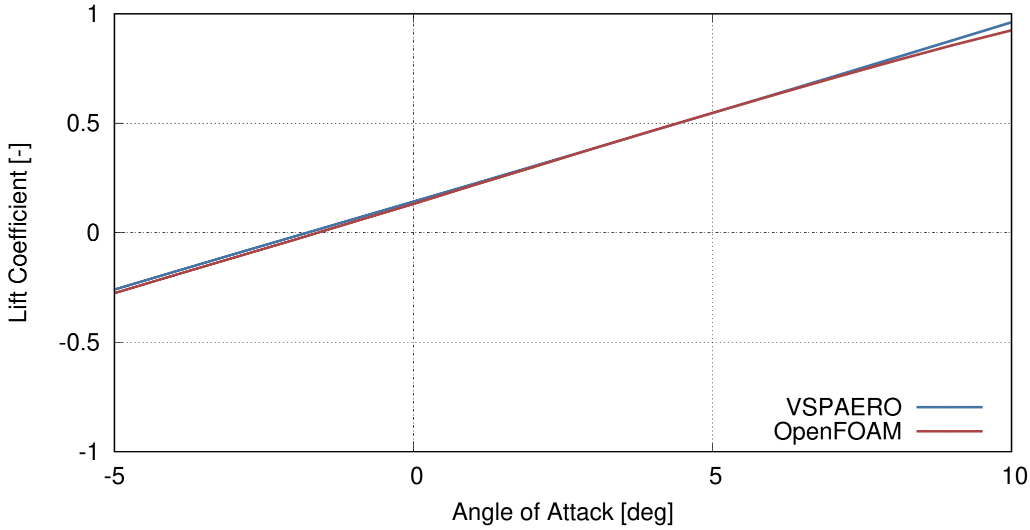

Figure 4.16: P-51 lift coefficient

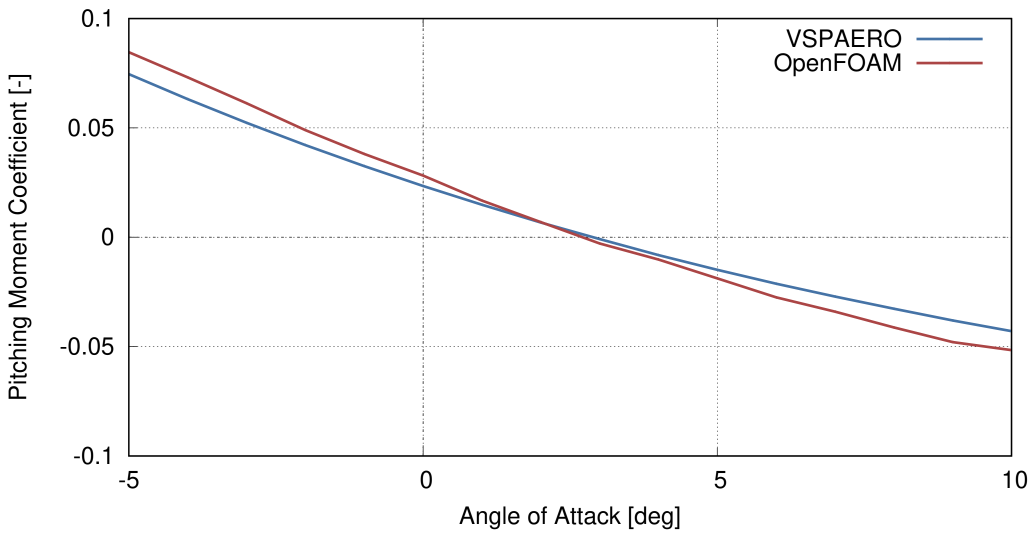

Figure 4.17: P-51 pitching moment coefficient

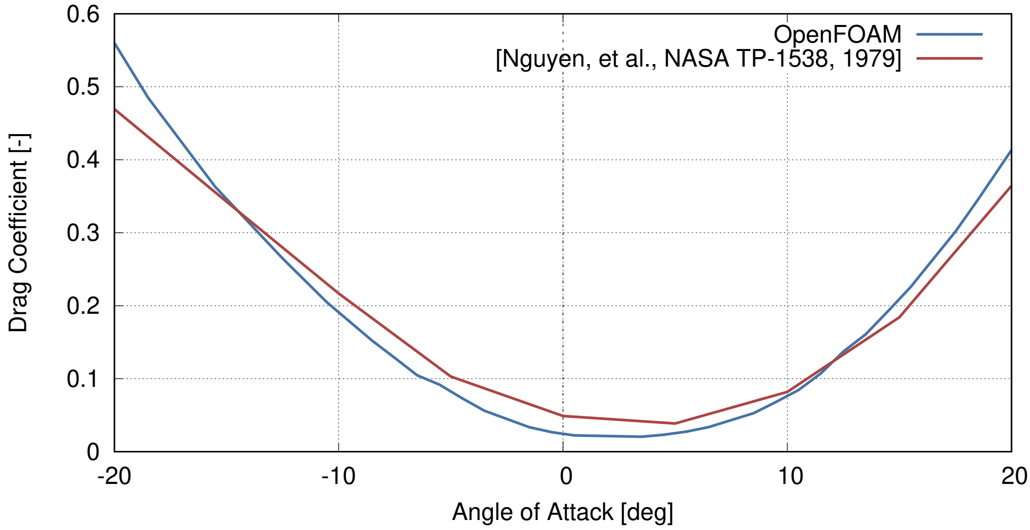

Figure 4.18: F-16 drag coefficient

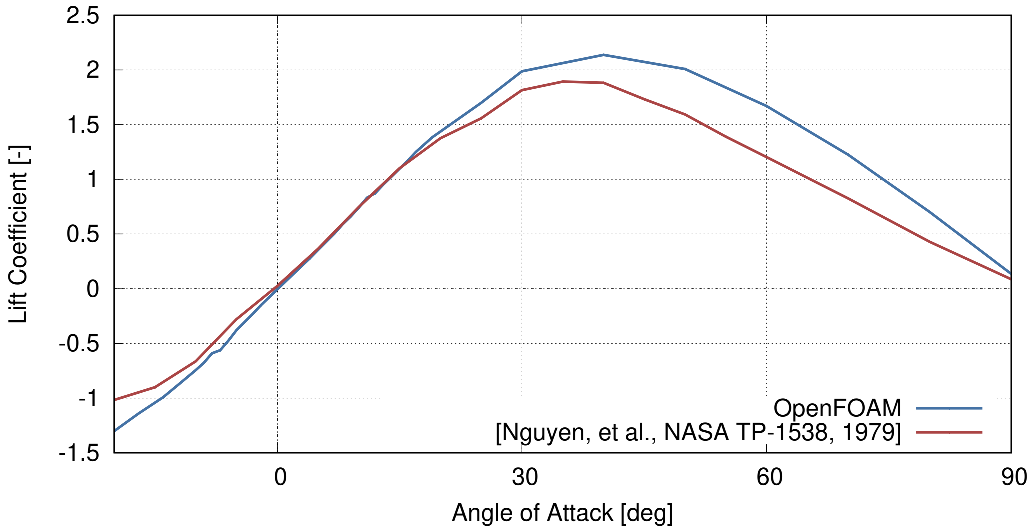

Figure 4.19: F-16 lift coefficient

Chapter 5

System Identification

System identification can be defined as the deduction of system characteristics from measured data. [22] Process of system identification includes performing identification experiment to obtain data, determining an appropriate form of the model and estimating the unknown parameters of the model with some statistically based method. [23]

5.1 Least Squares Method

Bibliography

[1] D. P. Raymer, *Aircraft Design: A Conceptual Approach.* American Institute of Aeronautics and Astronautics, 1992.

[2] T. C. Corke, *Design of Aircraft.* Pearson Education, 2003.

[3] C. Galinski, *Wybrane zagadnienia projektowania samolotow.* Wydawnictwa Naukowe Instytutu Lotnictwa, 2016. [in Polish].

[4] Z. Paturski, *Przewodnik po projektach z Mechaniki Lotu, Projekt nr 2: Charakterystyki aerodynamiczne plata.* [in Polish].

[5] E. Torenbeek, *Synthesis of Subsonic Airplane Design.* Delft University Press, 1982.

[6] M. D. Takahashi, *A Flight-Dynamic Helicopter Mathematical Model with a Single Flap-Lag-Torsion Main Rotor.* National Aeronautics and Space Administration, TM-102267, 1990.

[7] C. C. Critzos, H. H. Heyson, and R. W. Boswinkle, *Aerodynamic Characteristics of NACA 0012 Airfoil Sections at Angles of Attack from 0 to 180.* National Advisory Committee for Aeronautics, TN-3361, 1955.

[8] R. E. Sheldahi and P. C. Klimas, *Aerodynamic Characteristics of Seven Symmetrical Airfoil Sections Through 180-Degree Angle of Attack for Use in Aerodynamic Analysis of Vertical Axis Wind Turbines.* Sandia National Laboratories, 1981.

[9] Z. Paturski, *Przewodnik po projektach z Mechaniki Lotu, Projekt nr 9: Rownowaga podluzna samolotu i sily na sterownicy wysokosci.* [in Polish].

[10] B. Litherland, "Using VSPAERO," 2015. [Accessed 2019-01-20]. Available from: `http://openvsp.org/wiki/doku.php?id=vspaerotutorial`.

[11] M. Drela and H. Youngren, "XFOIL 6.9 User Primer," 2001. [Accessed 2019-01-20]. Available from: `https://web.mit.edu/drela/Public/web/xfoil/xfoil_doc.txt`.

[12] B. Litherland, "Modeling for VSPAERO," 2015. [Accessed 2019-05-12]. Available from: `http://openvsp.org/wiki/doku.php?id=vspaeromodeling`.

[13] C. J. Greenshields, *OpenFOAM User Guide version 6*, 2018.

[14] F. Moukalled, L. Mangani, and M. Darwish, *The Finite Volume Method in Computational Fluid Dynamics, An Advanced Introduction with OpenFOAM and Matlab.* Springer International Publishing, 2016.

[15] H. K. Versteeg and W. Malalasekera, *An Introduction to Computational Fluid Dynamics, The Finite Volume Method.* Pearson Education Limited, 2007.

[16] "OpenFOAM: User Guide: k-omega Shear Stress Transport (SST)," 2019. [Accessed 2019-05-19]. Available from: `https://www.openfoam.com/documentation/guides/latest/doc/guide-turbulence-ras-k-omega-sst.html`.

[17] B. Andersson, R. Anderssin, L. Hakansson, M. Mortensen, R. Sudiyo, and B. van Wachem, *Computational Fluid Dynamics for Engineers.* Cambridge University Press, 2012.

[18] J. H. Ferziger and M. Peric, *Computational Methods for Fluid Dynamics.* Springer-Verlag, 2002.

[19] *ANSYS Fluent User's Guide, Release 15.0*, 2013.

[20] J. Guerrero, "Tips and tricks in OpenFOAM," 2018. [Accessed 2019-05-19]. Available from: `http://www.wolfdynamics.com/wiki/OFtipsandtricks.pdf`.

[21] L. T. Nguyen, M. E. Ogburg, W. P. Gilbert, K. S. Kibler, P. W. Brown, and P. L. Deal, *Simulator Study of Stall/Post-Stall Characteristics of a Fighter Airplane With Relaxed Longitudinal Static Stability.* National Aeronautics and Space Administration, TP-1538, 1979.

[22] R. E. Maine and K. W. Iliff, *Identification of Dynamic Systems: Theory and Formulation.* National Aeronautics and Space Administration, RP-1138, 1985.

[23] T. Soderstrom and P. Stoica, *System Identification.* Prentice Hall, 1989.